

# Status of the Electroweak Standard Model

D. Haidt  
 DESY

## 1 INTRODUCTION

The simple  $SU(2) \otimes U(1)$  electroweak theory impresses by its uninterrupted series of successes when confronted with experiments. The crucial discovery of weak neutral currents in *Gargamelle* 1973 paved the way to this type of theoretical models as opposed to models with heavy gauge leptons. Further neutrino experiments and the observation of a parity violating asymmetry in *ed* scattering filtered out from the variety of competing models, in only six years or so, the one which became then the *Standard Model*.  $e^+e^-$  experiments at PETRA, PEP and TRISTAN extended the range of validity into the  $Q^2$  range on the order of  $10^3 \text{ GeV}^2$ . The  $S\bar{p}\bar{p}$ S collider experiments have observed, 10 years after the discovery of weak neutral currents, the heavy

gauge bosons with mass values as anticipated on the basis of low energy measurements.

At the present time (spring 1989) the whole body of experimental data spanning many orders in  $Q^2$  is well described by the electroweak standard model. This is a great success. However, the individual experiments are usually of moderate precision. This situation invited several groups to combine all the available data belonging to the same type, i.e. low energy fixed target experiments,  $e^+e^-$  experiments and  $p\bar{p}$  experiments, and to perform various types of fits. Table 1 collects recent reviews.

It is the aim of this report to confront the results extracted from the experiments in each sector with

| Authors   | Publication                   | Data                                       | Subjects   |
|---|-------------------------------|--|--|
| Amaldi, Böhm, Durkin, Langacker, Mann, Marciano, Sirlin, Williams | PR D36 (1987) 1385            | NC<br>W, Z<br>(no $e^+e^-$ )               | Fits : sectorwise, $\sin^2\Theta_W$ , $\rho$ and $\sin^2\Theta_W$ ; u,d,e weak couplings, QFD quantum level tests ; $m_t$ limits ; new physics |
| Costa, Ellis, Fogli, Nanopoulos, Zwirner                          | NP B297 (1988) 244            | NC<br>W, Z<br>(no $e^+e^-$ )               | as above   |
| Fogli   | EPL 4 (1987) 527              | all $\nu, \bar{\nu}e$                      | $e_R, e_L$ ; $\sin^2\Theta_W$  |
| Fogli and Haidt   | ZP C40 (1988) 379             | all $\nu, \bar{\nu}q$                      | $u_R^2, u_L^2, d_R^2, d_L^2$ ; $m_c$ ; $m_t$ limit<br>$\sin^2\Theta_W$   |
| Haidt and Pietschmann   | Landolt-Börnstein I/10 (1988) | all  | Systematic presentation of all electroweak data<br>many QFD tests  |
| Ellis and Fogli   | PL 213 B (1988) 526           | NC, W, Z                                   | $m_t$ dependent fits to each sector  |
| Einsweiler  | CERN 1988                     | W, Z                                       | Masses, $\Delta r$ , $\sin^2\Theta_W$  |
| Marshall  | ZP C43 (1989) 607             | $e^+e^-$<br>$\sqrt{s} \leq 52 \text{ GeV}$ | $a_l, v_l (l = e, \mu, \tau)$ ; $a_c, a_b$<br>$\sin^2\Theta_W$ ; $\alpha_s$  |
| Fogli   | BARI 40/89 (2/1989)           | NC, W, Z<br>(no $e^+e^-$ )                 | Electroweak radiative corrections  |
| Langacker   | HEP 1988 München              | all  | Status of QFD uniqueness   |

Table 1: Very recent review articles

the electroweak standard model in its minimal form (QFD), to search for internal inconsistencies and, if not found, to obtain best values for the electroweak couplings together with constraints on the as yet unobserved top quark. The material in the reviews of Table 1 is freely used and quoted by mentioning just the names. The  $e^+e^-$  data of the three TRISTAN experiments, even though partly preliminary, are now systematically included in the fits.

## 2 THE THEORETICAL FRAMEWORK

### a The free parameters

The Lagrangian of QFD can be grouped into a free part and three terms responsible for the interactions of the gauge bosons amongst themselves, the interactions of a gauge boson with fermion-antifermion pairs and the interactions involving Higgs bosons. This is schematically illustrated in Table 2 (see e.g. Haidt and Pietschmann). Some of the parameters appearing in the electroweak Lagrangian are related. Table 3 (see e.g. Haidt and Pietschmann) lists an independent subset. For actual calculations a renormalization scheme must be chosen. In essence, each parameter of the theory is determined by an experimental procedure which fixes both the numerical value and the energy scale associated. Amongst the parameters two are related to the group structure of the theory, namely :

$$g = \frac{e}{\sin\Theta_W} \quad g' = \frac{e}{\cos\Theta_W}$$

and two others are needed to fix the Higgs potential being chosen to be the mass  $m_H$  of the Higgs scalar particle and the vacuum expectation value  $\lambda$  of the Higgs field (see e.g. Hollik [4]). The three couplings in Table 3 are defined as follows :

#### • $\alpha$

The defining relation for  $\alpha$  is the Thomson cross section

$$\sigma_{Thomson} = \frac{8\pi\alpha^2}{3m^2}$$

| Part                                     | Interaction  | Parameters   | Constraints  |
|--|--|--|--|
| $\mathcal{L}_0$                          | free   | $m_f$<br>$m_\gamma, m_W, m_Z$<br>$m_H$   | $m_\nu=0$<br>$m_\gamma=0$<br>$m_W = \frac{1}{2}g\lambda, m_Z = \frac{m_W}{\cos\Theta_W}$ |
| $\mathcal{L}_{GB}$                       | Z W W<br>$\gamma$ W W  | $g \cos\Theta_W$<br>$g \sin\Theta_W$   | $e = g \sin\Theta_W$   |
| $\mathcal{L}_{em}$<br>$\mathcal{L}_{CC}$ | $\gamma f\bar{f}$<br>W $f'\bar{f}$                                       | $e, Q_f$<br>$g, U_{q'q}$<br>$v_f^{CC}, a_f^{CC}$   | $Q_f = 0, \pm\frac{1}{3}, \pm\frac{2}{3}, \pm 1$<br>$v_f^{CC} = a_f^{CC} = 1$            |
| $\mathcal{L}_{NC}$                       | Z $f\bar{f}$   | $\frac{g}{\cos\Theta_W}, v_f, a_f$   | $v_f = T_3^L - 2Q_f \sin^2\Theta_W$<br>$a_f = T_3^L$                                     |
| $\mathcal{L}_H$                          | H W W<br>H Z Z<br>H $f\bar{f}$<br>H H H<br>H H H H<br>H H W W<br>H H Z Z | $g^4\lambda$<br>$g^4\lambda/\cos\Theta_W$<br>$m_f/\lambda$<br>h $\lambda$<br>h<br>$g^4$<br>$g^4$ | $2h\lambda^2 = m_H^2$  |

Table 2: The electroweak Lagrangian

|                    |  |
|--------------------|--|
| <b>Masses :</b>    | $m_e, m_\mu, m_\tau$<br>$m_d, m_s, m_b$<br>$m_u, m_c, m_t$<br>$m_H$ (Higgs mass)     |
| <b>Mixing :</b>    | $\theta_1, \theta_2, \theta_3, \delta$<br>(Kobayasi-Maskawa matrix)                  |
| <b>Couplings :</b> | $\alpha$ (finestructure constant)<br>G (Fermi coupling constant)<br>$\sin^2\Theta_W$ |

Table 3: Set of independent electroweak parameters

$\alpha$  and  $e$  are related through  $e^2 = 4\pi\alpha$  ; the present best value of alpha is  $\alpha^{-1} = 137.035989 \pm 0.0000061$ .

#### • G

G sets the Fermi scale. It is related to  $\lambda$  through :  $G^{-1} = \sqrt{2}\lambda^4$ . The defining relation for G is the muon lifetime :

$$\Gamma(\mu \rightarrow e\bar{\nu}_e\nu_\mu) = \frac{m_\mu^5 G^2}{192\pi^3} \left(1 - \frac{8m_e^2}{m_\mu^2}\right) \left(1 + \frac{\alpha}{2\pi} \left(\frac{25}{4} - \pi^2\right)\right)$$

Numerically,  $G = (1.16637 \pm 0.00001) 10^{-5} / G_e V^2$ .

#### • $\sin^2\Theta_W$

The quantity  $\sin^2\Theta_W$  is defined by :

$$\sin^2\Theta_W = 1 - \frac{m_W^2}{m_Z^2}$$

Here  $m_W$  and  $m_Z$  are the physical masses of the weak gauge bosons. Therefore, an equivalent choice would be to take as independent  $\alpha$ ,  $G$  and  $m_Z$  for instance. As opposed to the definition of  $\alpha$  and  $G$ , which refer to  $Q^2 \approx 0$ ,  $\sin^2\Theta_W$  is defined at the scale of the weak gauge boson masses. A value for  $\sin^2\Theta_W$  is obtained by comparing theoretical predictions with experimental measurements from low energy fixed target experiments,  $e^+e^-$  and  $p\bar{p}$  experiments (see the next sections).

## b The Task

QFD is a renormalizable theory, this means *any* experimental electroweak quantity can be predicted theoretically in terms of a *finite* number of parameters, i.e.  $p_1, p_2, \dots, p_{17}$  of Table 3. These parameters are known with some precision from a priori determinations. Therefore a new measurement leads to the following situation :

$$\begin{aligned} \text{Measurement} &: Q^{exp} \pm \Delta Q^{exp} \\ \text{Theory} &: Q^{theor}(\vec{p} \pm \Delta\vec{p}) \end{aligned}$$

If the theoretical prediction agrees with the experimental measurement, then the new experimental datum can be used to constrain further the theoretical input parameters. In the other case, the new measurement (if confirmed by others) would reveal an inconsistency within the theoretical framework under consideration and would point to new physics.

## c Prediction of the W-mass

Given the above renormalization scheme the mass of the charged weak gauge boson can be predicted :

$$\begin{aligned} m_W &= f(\alpha, G, \sin^2\Theta_W, m_f, m_H) \\ &= \sqrt{\frac{\pi\alpha}{\sqrt{2}G} \frac{1}{\sin\Theta_W} \frac{1}{\sqrt{1 - \Delta r(\alpha, G, m_t, \dots)}}} \\ &= \frac{37.281 \text{ GeV}}{\sin\Theta_W} \frac{1}{\sqrt{1 - \Delta r(\alpha, G, m_t, \dots)}} \quad (5) \end{aligned}$$

This relation was derived by Sirlin [5] 1980. Its structure is simple. The first part represents the lowest order prediction of the mass depending only upon  $\alpha, G, \sin^2\Theta_W$ , whereas the last term accounts for the effect of electroweak radiation and depends upon the full parameter set. The size of  $\Delta r$  is sensitive to the mass of the as yet unobserved top quark, as displayed in Figure 1 (calculated with the program of Hollik and Burgers). The dependence of  $\Delta r$  on the Higgs mass is rather weak over the range  $10 \leq m_H \leq 1000$  GeV. For this reason the Higgs mass is kept fixed at 100 GeV. A precise measurement of  $\sin^2\Theta_W$  and  $m_W$  in independent experiments represents therefore a test of QFD at the quantum loop level. This was an important motivation for the last round of neutrino experiments at CERN [2].

A historical note : Only three years after the discovery of weak neutral currents the value of  $\sin^2\Theta_W$  deduced from the first neutrino experiments was applied to predict (in lowest order) the mass of the W boson around 70 GeV. It was then clear, that no existing machine would allow the direct production of intermediate vector bosons. At the Aachen Conference 1976

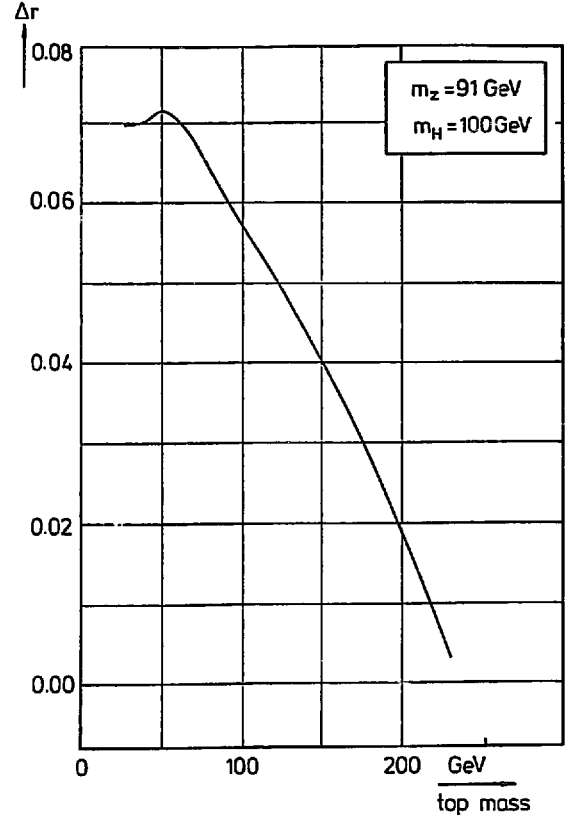


Figure 1:  $\Delta r$  versus  $m_t$  for  $m_Z = 91$  GeV and  $m_H = 100$  GeV

a proposal of a  $p\bar{p}$  collider was discussed, which would provide enough energy to generate real  $W$ 's. Seven years later this ambitious goal was achieved.

### 3 THE GAUGE BOSON SECTOR

#### a Direct mass measurements

| Experiment | W                      | Z                      | Reference |
|------------|------------------------|------------------------|-----------|
| UA 1       | $82.7 \pm 1.0 \pm 2.7$ | $93.1 \pm 1.0 \pm 3.1$ | Table 1   |
| UA 2       | $80.2 \pm 0.6 \pm 1.4$ | $91.5 \pm 1.2 \pm 1.7$ | Table 1   |
| CDF        | $80.0 \pm 3.3 \pm 2.4$ |                        | [1]       |
| Average    | $80.7 \pm 1.3$         | $91.6 \pm 1.6$         |           |

Table 4: Gauge boson masses (in GeV)

All published data from the  $p\bar{p}$  colliders are summarized in Table 4. In obtaining the averages the correlations are taken into account. The result is conveniently illustrated in the  $(m_Z, m_Z - m_W)$  plane (see Figure 2). The interpretation within QFD is straightforward :

$$\begin{aligned} \sin^2 \Theta_W &= 1 - \left(\frac{m_W}{m_Z}\right)^2 = \\ &= 0.222 \pm 0.020 \\ \Delta r &= 1 - \left(\frac{37.281 \text{ GeV}}{m_W}\right)^2 / \left(1 - \left(\frac{m_W}{m_Z}\right)^2\right) = \\ &= 0.03 \pm 0.08 \end{aligned}$$

applying the definition of  $\sin^2 \Theta_W$  and the Sirlin relation (1). Figure 3 displays the lines of constant  $\sin^2 \Theta_W$  and  $\Delta r$  in the  $(m_Z, m_Z - m_W)$  plot.

#### b The Z-propagator in $e^+e^-$

Due to the  $(\gamma, Z)$ -interference terms of the form

$$\left(1 - \frac{s}{m_Z^2}\right)^{-1}$$

are appearing in the expressions for the asymmetry  $A_f$  and the total cross section  $R_f$  in the process  $e^+e^- \rightarrow f\bar{f}$ . This term is numerically 1.8 for the highest energy so far reached at TRISTAN (60.8 GeV). A fit to all  $R_{had}$  data from PETRA, PEP and TRISTAN ranging from 14 up to 60.8 GeV yields  $m_Z$  to a precision of 1.4 GeV (see next chapter). The Z-propagator is also visible in the processes  $e^+e^- \rightarrow l\bar{l}$  ( $l = \mu, \tau$ ); the sensitivity to  $m_Z$  is, however, limited by statistics and therefore not considered further.

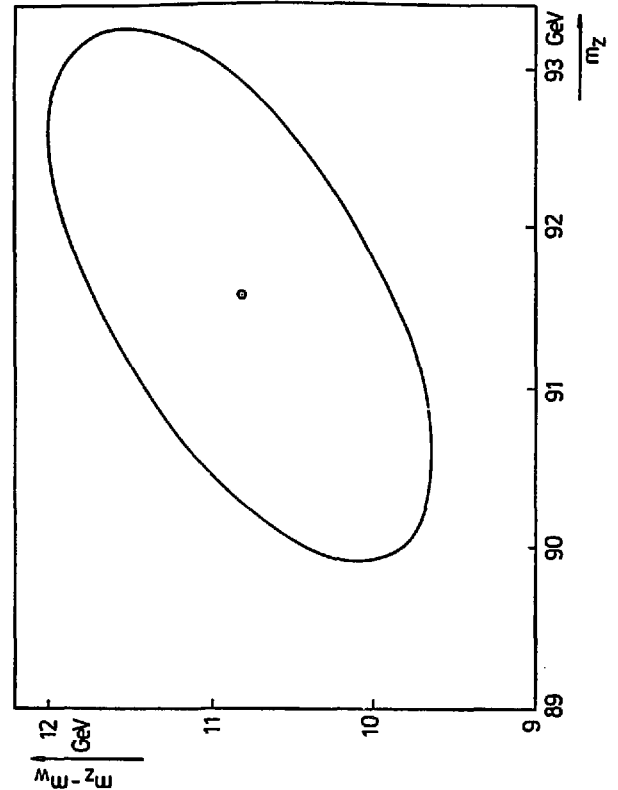


Figure 2: Data from UA1, UA2, CDF

#### c The W-propagator in deep inelastic $\nu q$ scattering

The total cross section of  $\nu q$  scattering is observed to increase linearly with increasing neutrino energy (see Figure 4 taken from Haidt and Pietschmann). The W-propagator causes a deviation from linearity. The absence of any observable deviation from linearity allowed to quote lower limits for the intermediate vector boson starting at order 1 GeV in the 60's, continuing up to order 10 GeV in the 70's and reaching order 50 GeV in the 80's until the direct observation in 1983 at the CERN  $p\bar{p}$  collider. The W propagator effect at the high energy end of the  $\nu N$  experiments amounts to less than one standard deviation.

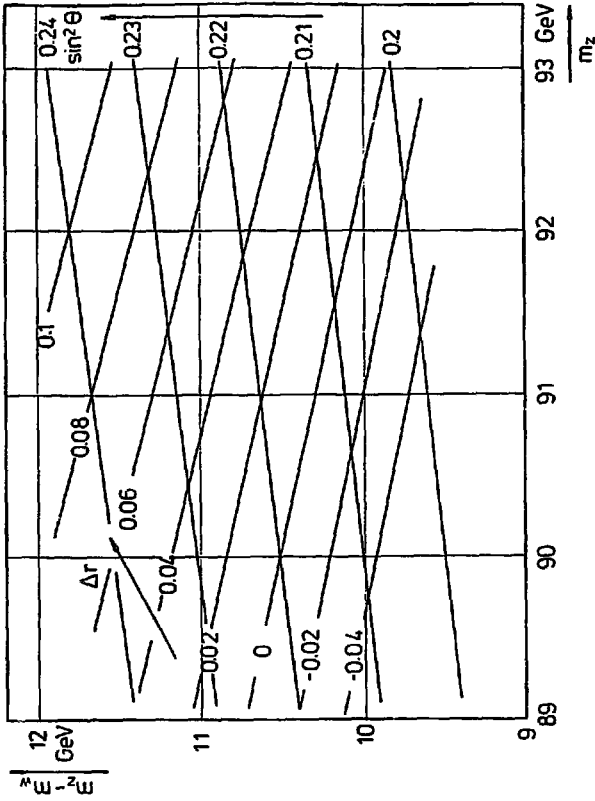


Figure 3: Lines of constant  $\sin^2\Theta_W$  and  $\Delta r$

## 4 THE $e^+e^-$ SECTOR

The evaluation of the process  $e^+e^- \rightarrow hadrons$  at the PETRA and PEP  $e^+e^-$  colliders provided a value of  $\sin^2\Theta_W$  together with the strong interaction coupling constant. The information on  $\sin^2\Theta_W$  comes mainly from the quark vector couplings. With the advent of the TRISTAN  $e^+e^-$  collider the Z propagator can be measured directly due to the much higher centre of mass energy. These new measurements constitute a significant test of QFD.

### a Formulae

The electroweak cross section of the process  $e^+e^- \rightarrow f\bar{f}$  in terms of  $\sigma_\mu = \frac{4\pi\alpha^2}{3s}$  in lowest order is given by :

$$R_f = Q_f^2 Q_f^2 + 2v_e v_f R_e \chi(s) + (v_e^2 + a_e^2)(v_f^2 + a_f^2) |\chi(s)|^2$$

and exhibits the pure QED term, the electroweak interference term and the purely weak term with their characteristic energy dependence. The function  $\chi$  depends upon the ratio of the  $\gamma$ - and Z-propagators as well as on the electroweak coupling parameters :

$$\begin{aligned} \chi(s) &= \frac{1}{(\sin 2\Theta)^2} \frac{s}{s - m_Z^2 + i\Gamma_Z m_Z} \\ &= -\frac{\sqrt{2}G}{4\pi\alpha} (1 - \Delta r) \frac{s}{1 - s/m_Z^2 - i\Gamma_Z/m_Z} \end{aligned} \quad (2)$$

In both expressions  $m_Z$  is the physical Z mass. The second equal sign follows from the application of the Sirlin relation (1). It is most important that now the very precise ratio  $G/\alpha$  is occurring together with the quantity  $\Delta r$  which contains amongst other quantities the mass of the top-quark.

It goes by itself, that the measured quantity  $R_{had}$  can only be confronted to  $\sum_q R_q$  (q running over all active flavours, i.e. u,d,s,c,b) after taking into account electroweak radiative effects, which themselves depend upon quantities like  $m_Z$  and  $m_t$ , and QCD radiative effects. This makes the consideration of electroweak radiative effects a central issue.

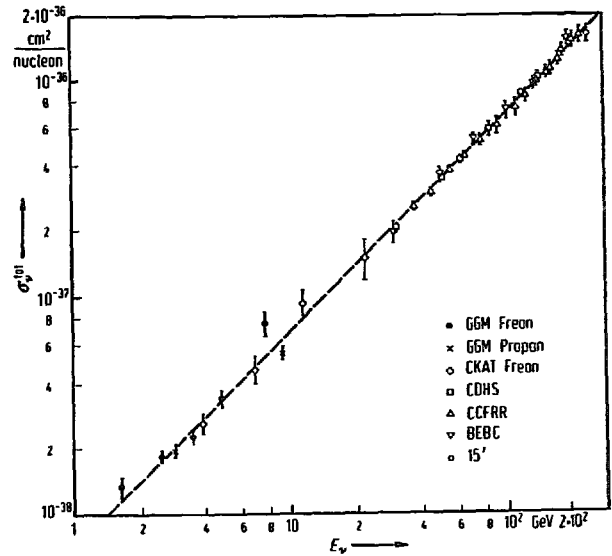


Figure 4: Total cross section vs.  $E_\nu$

## b Radiative effects in $R_{had}$

Multihadron events due to  $e^+e^- \rightarrow hadrons$  are easy to recognize in the omnipurpose detectors at the  $e^+e^-$  colliders except, of course, near to the forward and backward direction due to the beampipe. A cut in the observed total energy ensures that the events are predominantly arising from single photon or Z exchange. The observed events include radiative effects from QED, purely weak and strong interactions.

The published quantity is obtained as follows :

$$R_{had} = \frac{N}{L\sigma_\mu\epsilon(1+\delta)}$$

where  $N$  is the observed number of events within the acceptance cuts after subtracting the small background,  $L$  the integrated luminosity,  $\epsilon$  the detector acceptance and  $\delta$  the correction factor due to electroweak radiative effects. The reference cross section is  $\sigma_\mu = \frac{4\pi\alpha^2}{3s}$ . QCD effects are not corrected for.

Published R-values from different experimental group can usually not be compared with each other. The reason is that there is no unanimous agreement on what part of the electroweak effects should be corrected for. Furthermore, the result depends upon the choice of electroweak parameters used to calculate the radiative effects.

The evaluation of  $R$  involves two experimental numbers ( $N$  and  $L$ ), all the rest requires calculations based on the electroweak theory and knowledge about the detector. In the past frequent use has been made of the program by Berends, Kleiss and Jadach (BKJ), which provides only partial account of the electroweak 1-loop contributions. Recently, programs with full electroweak corrections up to  $O(\alpha^3)$  have become available. Figure 5 shows the relevant graphs grouped into two categories( from [4]) :

- Category 1 is marked out as a gauge invariant subset dealing with QED effects and accounts numerically for most of the contribution to  $\delta$ . The contributing diagrams arise from the Born graphs by adding an extra photon to them either as a

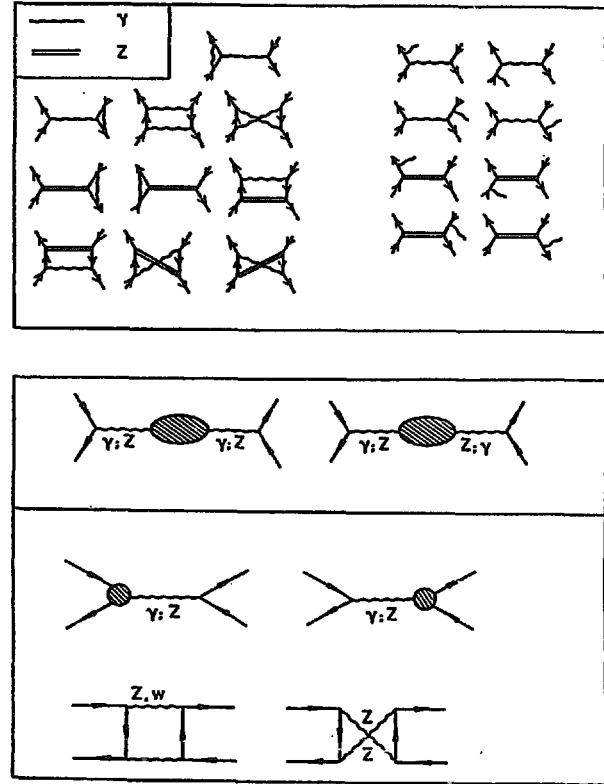


Figure 5: 1-loop diagrams

real bremsstrahlung or a virtual photon loop. It depends upon the detector acceptance cuts. This category is considered physically trivial. In the calculation enters the mass of the Z boson via the Z-exchange diagrams. This contribution is s-dependent.

- Category 2 consists of the nontrivial weak effects. It handles the propagator effects, where fermion loops, notably the topquark, enter, furthermore the vertex corrections and box contributions. These contributions do not depend upon the detector acceptance. They are relevant, if  $R_{had}$  is used to constrain electroweak parameters.

It seems natural to publish fully corrected data. Then, however, the result is valid only for the values of  $m_Z$  and  $m_t$  chosen a priori and the confrontation with theory must be done with just the same parameter values. In other words, the same data corrected with a different choice of  $m_Z$  and  $m_t$  would yield a numerically different result. This is quite inconvenient, if the published R-value is to be used to extract information on electroweak parameters.

An alternative way would be to publish  $R$  corrected only for the trivial QED diagrams of category 1. It is then assured that the result is detector independent, but also the nontrivial propagator effects, particularly the full top mass dependence, remain in the published quantity, denoted  $R_{ew}$ , rather than being divided out as a correction. The advantage of  $R_{ew}$  as opposed to  $R_{Born}$  is illustrated in Figure 6. Most striking is its property to be very little dependent upon the top mass. This can be traced back to the appearance of the Z-propagator selfenergy term compensating partially the  $m_t$  dependence of the term  $1 - \Delta r$  (see [4]).

### c Results

There exist excellent reviews of the PETRA and PEP data. The latest summary of Marshall (see Table 1) analyzing the  $R_{had}$  values (including the published TRISTAN points at 50 and 52 GeV) yields :

$$\sin^2 \Theta_W = 0.236 \pm 0.015$$

This result was obtained by fitting simultaneously  $\sin^2 \Theta$  and  $\Lambda$  assuming  $\Delta r = 0.071$  (corresponding to  $m_t \approx 45$  GeV). The systematic error in  $\Delta R/R$  is smaller than 1 % as a result of intense efforts of the collaborations over many years. A glance at the theoretical expression of  $R$  shows that for centre of mass energies in the PETRA range the sensitivity to the propagator term is almost negligible. The information on  $\sin^2 \Theta_W$  is derived essentially from the weak vector couplings of the quark mixture.

The TRISTAN data now available up to 60.8 GeV change the situation dramatically. The Z-propagator effect is seen in Figure 7 as a prominent rise. The weighted statistical  $R_{ew}$  data together with the theoretical expectation for  $m_Z = 89$  GeV and 90 GeV are shown. The data of all groups agree at almost all energies within one standard deviation. Large statistical fluctuations, as may be expected among 30 independent points, do not occur. Each of the three groups evaluated systematic errors between 4 and 5 %. These errors are not independent of each other, since for instance the same or similar programs have been applied in order to evaluate the radiative effects and the detector acceptance. To be definite I assume a 2 % irreducible systematic error common to all three experiments. The consequence of this is that the Z mass derived from the data has an induced systematic uncer-

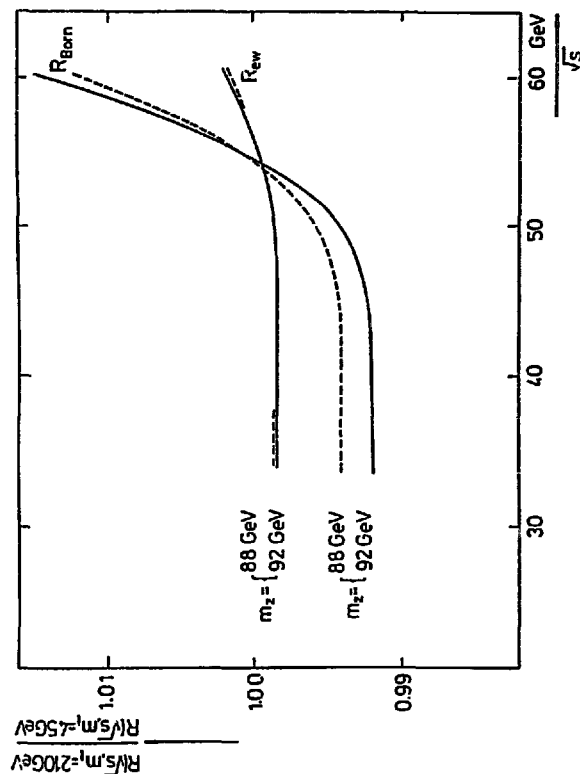


Figure 6:  $R_{ew}$  vs  $R_{Born}$

tainty of 1.1 GeV. Each experimental group provided *fully corrected* [6] points either in published form or in preliminary graphical form presented to recent conferences [7] (Moriond, updates at this Workshop and the KEK Symposium in May 1989). In order to combine the data and confront them with the theoretical expectation I have them transformed into  $R_{ew}$  by multiplying them with the ratio  $R_{ew}/R_{Born}$  calculated with the program of Hollik and Burgers applying exactly the same a priori values for  $m_Z$  and  $m_t$  as each group assumed for their calculation of the radiative corrections. The fit of  $m_Z$  to these quantities is then easily performed, since it is *almost independent of the top mass*, as long as it is not much larger than 250 GeV. It is interesting to note that the  $s$ -dependence of  $R$  (i.e. slope and curvature), which is much less sensitive to systematic uncertainties than the absolute  $R$ -values, provides a quite significant constraint. The electroweak theory describes the data well over the full energy range. There is in particular no indication of an increased rise in  $R$  as should be expected from a top quark of mass below and near to 30 GeV. This is confirmed by inspecting differential distributions such as the thrust or the aplanarity

distributions.

The fit result is :

$$m_Z = 89.2 \pm 1.2 \pm 1.1 \text{ GeV}$$

where the first error is due to the experimental uncertainty (statistical and independent systematic errors averaged over all three experiments), whereas the second error reflects the irreducible overall uncertainty. The statistical error is much smaller than the systematic one. A more elaborate treatment of systematic errors in the fit must wait until the experimental analyses are finalized.

When combining the PETRA/PEP with the TRISTAN data a small common systematic uncertainty was allowed for. It is the tremendous increase in sensitivity with the centre of mass energy  $\sqrt{s}$  that makes the TRISTAN experiments contribute as much as the PETRA/PEP experiments with only 10 % of the statistics.

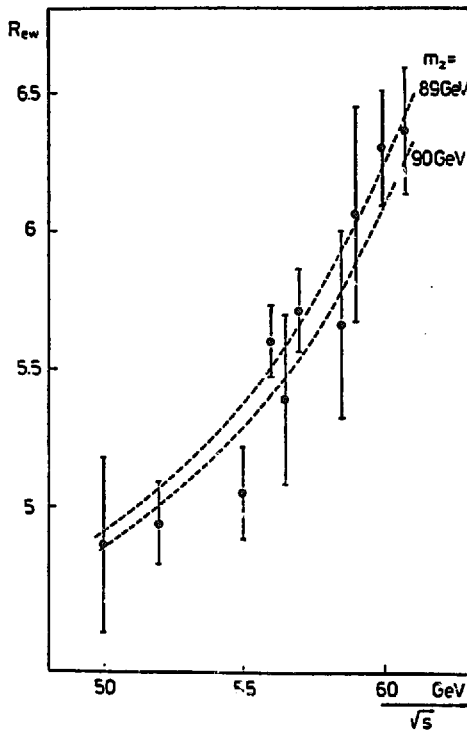


Figure 7: TRISTAN R-data and theoretical expectation for 89 and 90 GeV

The results from the  $e^+e^-$  and the  $p\bar{p}$  sectors agree well with each other and can be combined. The combined constraint in the  $(m_Z, m_Z - m_W)$  plane is shown in Figure 8.

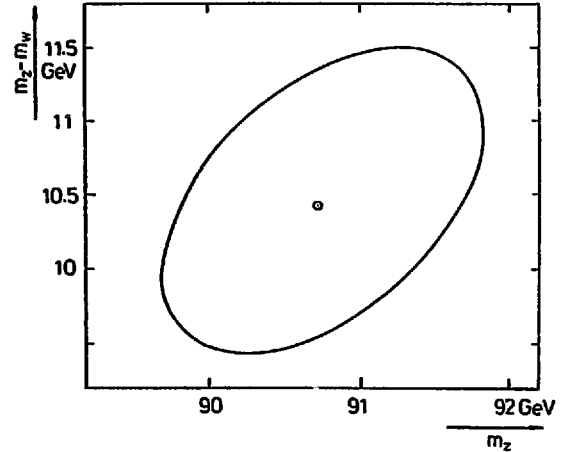


Figure 8: Combination of the  $e^+e^-$  and  $p\bar{p}$  sectors

## 5 Fixed target experiments

### a Deep inelastic $\nu N$ scattering

Neutrino experiments have played a pilot role in the understanding of weak phenomena. The value for  $\sin^2\Theta_W$  deduced from the large amount of measurements in  $\nu$  and  $\bar{\nu}$  nucleon experiments from 1973 until 1988 is still the most precise one. The method consists basically in measuring in each experiment simultaneously the total cross sections of the neutral current (NC) and charged current (CC) induced processes and forming the ratio NC/CC. This ratio contains information on the weak  $Z^0 u\bar{u}$  and  $Z^0 d\bar{d}$  couplings and has the advantage that many sources of systematic errors drop out or are at least considerably reduced. In view of the direct mass measurements at the CERN  $p\bar{p}$  collider in a Workshop end 1982 the challenging precision of  $\pm 0.005$  [2] in a  $\nu$  experiment was put forward as a test of QFD at its quantum level. Four  $\nu$  experiments came close to this ambitious goal pushing thus the experimental technique to its limit.

The ingredients for the extraction of the weak u and d couplings can be seen from the diagram in Figure 9.



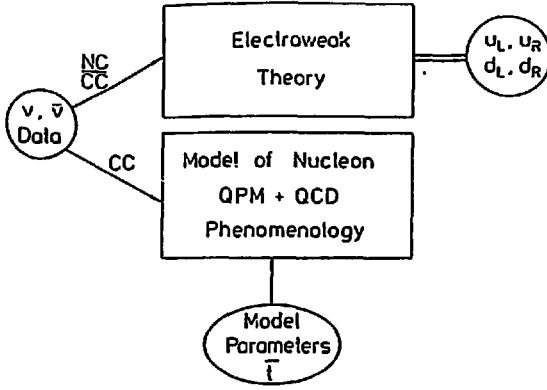


Figure 9: Procedure to determine the weak couplings

| Coupling         | Value  | $\sigma_{exp}$ | $\sigma_{syst}$ |
|------------------|--------|----------------|-----------------|
| $u_L^2$          | 0.1197 | 0.0116         | 0.0008          |
| $d_L^2$          | 0.1785 | 0.0119         | 0.0035          |
| $u_R^2$          | 0.0257 | 0.0081         | 0.0014          |
| $d_R^2$          | 0.0052 | 0.0078         | 0.0030          |
| $\sin^2\Theta_W$ | 0.2309 | 0.0029         | 0.0024          |

Table 5: Results from  $\nu$  data assuming  $m_H = 100$  GeV,  $m_c = 1.5$  GeV and  $m_t = 36$  GeV

The  $\nu$  and  $\bar{\nu}$  data fulfil a double role : they provide the measurement of NC/CC and also the necessary knowledge on the nuclear structure. The following results are taken from the most recent review by Fogli and Haidt (see Table 1). After obtaining a satisfactory description of the most recent and most precise  $\nu$  and  $\bar{\nu}$  structure functions all 43 experimental NC data were interpreted *simultaneously* and fitted to the four weak couplings  $u_L, u_R, d_L, d_R$ , thus ensuring the smallest possible systematic uncertainty. Table 5 shows the results.

All couplings, even the righthanded ones, are de-

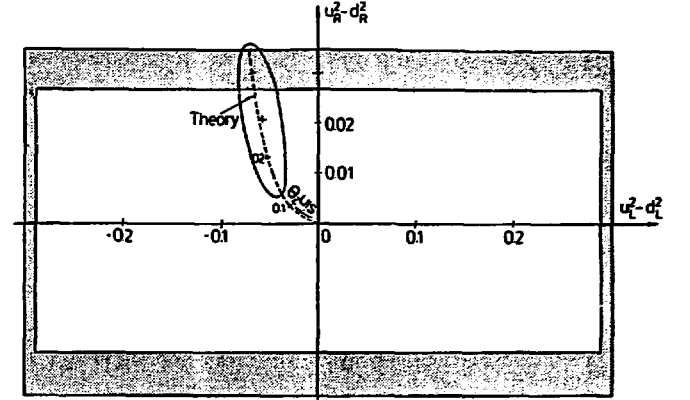


Figure 10: Test of QFD

cently measured. Figure 10 shows the constraint coming from the high precision calorimeter experiments measuring essentially the sums  $u_L^2 + d_L^2$  and  $u_R^2 + d_R^2$  (isoscalar targets). The inside of the open area gets constrained by the bubble chamber experiments, which allow separate measurements on protons and neutrons. The small allowed region agrees precisely with the QFD expectation.

The systematic error reflects the uncertainty in the input parameters of the phenomenological description of the nuclear model. The biggest uncertainty comes from the amount of sea quarks in the nucleon.

The above fit depends crucially upon the value of the charmed quark mass. The dependence arises from the charged current data. The phenomenological description of the transitions  $d \rightarrow c$  and  $s \rightarrow c$  is based on the *slow rescaling* scheme, which contains as external parameter the effective charmed quark mass. The structure functions in the  $\nu$  experiments were obtained with the choice  $m_c = 1.5$  GeV. A fit of the NC/CC data leaving  $\sin^2\Theta_W$  and  $m_c$  as free parameters is shown in Figure 11 and yields for  $m_c$  a value consistent with the a priori choice in the structure functions. The uncertainty of  $\pm 0.3$  GeV induces a shift in the value for  $\sin^2\Theta_W$  of  $\pm 0.004$ . This uncertainty limits the whole procedure. The final value for  $\sin^2\Theta_W$  integrating over  $m_c$  is :

$$\sin^2\Theta_W = 0.231 \pm 0.006$$

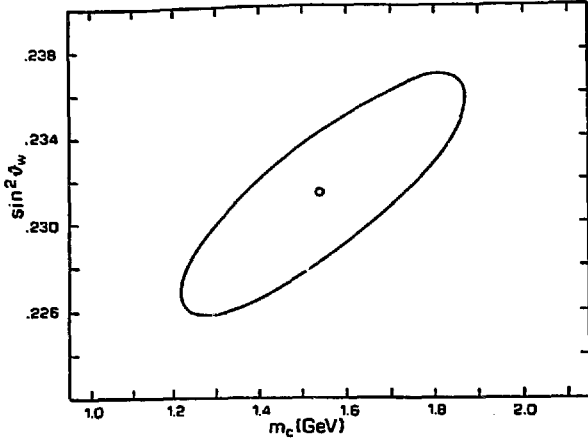


Figure 11: Simultaneous fit in  $\sin^2\Theta_W$  and  $m_c$  (1 st.dev. contour).

The top mass dependence is small due to compensating contributions in the radiative effects, unless  $m_t$  is much larger than 200 GeV. This is shown in Figure 12.

The precise value of  $\sin^2\Theta_W$  from all  $\nu q$  data agrees well with the  $p\bar{p}$  and  $e^+e^-$  data and reduces considerably the allowed region in the  $(m_Z, m_Z - m_W)$  plane as shown in Figure 13.

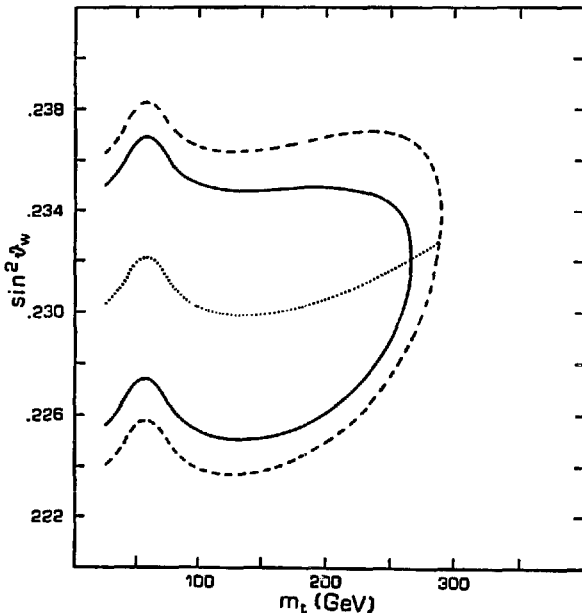


Figure 12: Simultaneous fit in  $\sin^2\Theta_W$  and  $m_t$  for  $m_c=1.5$  GeV. The solid (dashed) line takes the experimental (total) error into account

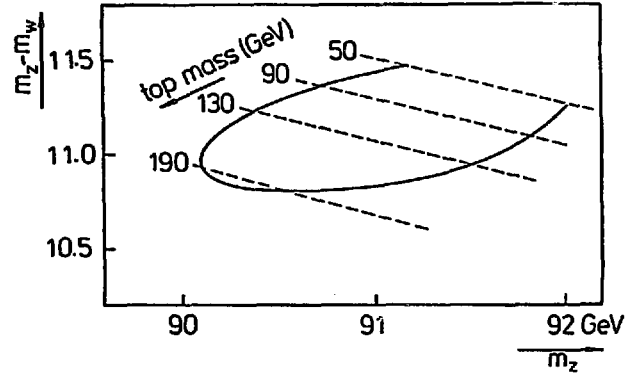


Figure 13: Combination of the  $p\bar{p}$ ,  $e^+e^-$  and  $\nu q$  sectors

## b $\nu e$ scattering

The two experiments, CHARM I at CERN and E 734 at BNL (see Table 6), have now final measurements of the total cross sections of  $\nu_\mu e$  and  $\bar{\nu}_\mu e$  scattering and also their ratio.  $\sin^2\Theta_W$  extracted from the ratio is insensitive to systematic errors. The result was obtained assuming  $m_t = 45$  GeV. Figure 14 from Ellis and Fogli shows how the extracted value for  $\sin^2\Theta_W$  changes with the assumed value for  $m_t$ .

| Experiment | $\nu_\mu e$ | $\bar{\nu}_\mu e$ | R               | $\sin^2\Theta_W$  |
|------------|-------------|-------------------|-----------------|-------------------|
| E 734      | 160         | 97                | $1.56 \pm 0.36$ | $0.197 \pm 0.025$ |
| CHARM I    | 83          | 112               | $1.20 \pm 0.35$ | $0.211 \pm 0.037$ |
| Average    |             |                   |                 | $0.201 \pm 0.021$ |

Table 6: Cross section ratio of  $\nu_\mu e$  and  $\bar{\nu}_\mu e$  scattering

Fogli has performed an analysis of all available  $\nu_\mu e$ ,  $\bar{\nu}_\mu e$ ,  $\nu_e e$  and  $\bar{\nu}_e e$  data and obtained for  $m_t = 90$  GeV :

$$\begin{aligned} e_L &= -0.273 \pm 0.018 \\ e_R &= +0.224 \pm 0.022 \end{aligned}$$

(3)

The correlation coefficient is 0.032. From the couplings  $\sin^2\Theta_W = 0.226 \pm 0.013$  is derived. This value includes the data of the CERN and BNL experiments, which so far are two most precise individual results. Within a few months the CHARM II collaboration will be able to provide a result with an anticipated precision of  $\pm 0.005$ . It remains to be seen whether the new data confirm the values of Table 6.

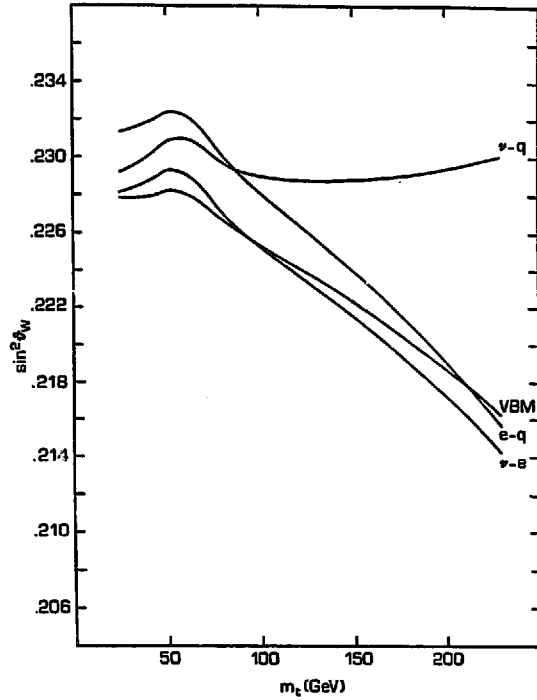


Figure 14:  $m_t$  dependence of the extracted  $\sin^2\Theta_W$

The LOS ALAMOS experiment yielded :

$$\sigma(\nu_e e)/E = (11.2 \pm 2.2 \pm 1.2) 10^{-42} \text{cm}^2/\text{GeV}$$

This result demonstrates the destructive interference of NC and CC in agreement with QFD. From the cross section follows  $\sin^2\Theta_W = 0.29 \pm 0.08$ .

### c eq-scattering

To this sector contribute the SLAC *ed* experiment (1978) the  $\mu C$  (Argento et al, 1983/4) and the atomic parity violation experiments. Among the latter important progress has been achieved by the Boulder group [3]. They obtained a rather precise value for the weak charge on caesium :

$$Q_w^{Cs} = -69.4 \pm 1.5 \pm 3.8$$

Note the small experimental error. Assuming  $m_t = 36$  GeV  $\sin^2\Theta_W$  of this single experiment is  $0.219 \pm 0.007 \pm 0.017$ . Averaging all Cs experiments of the Paris and Boulder groups one obtains

$$\sin^2\Theta_W = 0.220 \pm 0.015$$

where the error includes both the experimental and the theoretical uncertainties. The result is limited by uncertainties in atomic physics.

All data have been included in a simultaneous fit by Fogli (1989) with the result :

$$\begin{aligned} C_{1u} &= -0.209 \pm 0.047 \\ C_{1d} &= +0.358 \pm 0.042 \\ C_{2u} - \frac{1}{2}C_{2d} &= +0.002 \pm 0.188 \end{aligned}$$

The results from the  $\nu e$  and  $e q$  experiments agree well within their (still large) errors with the  $\nu q$  sector. The fixed target sector reduces further the region allowed in the  $(m_Z, m_Z - m_W)$  plane by the  $p\bar{p}$  and  $e^+e^-$  sectors, as shown in Figure 15.

## 6 CONCLUSIONS

The results within each sector and from sector to sector are in agreement. The  $e^+e^-$  sector has gained an impact on constraining electroweak parameters comparable to other sectors. The main conclusion is therefore that all data can *still* be consistently interpreted within the electroweak theory in its minimal form (QFD). The sequence of Figures 2,8,13,15 shows the impressive experimental progress as well as the status of the confrontation with theory. The fit assuming the Higgs mass fixed at 100 GeV constrained the two parameters  $m_Z$  and  $m_Z - m_W$  or equivalently  $\sin^2\Theta_W$  and  $m_t$  to a small area. A few remarks may be added :

- **Radiative effects**

The fit would be unacceptable without the inclusion of radiative electroweak effects.

- **Top**

The mass of the top quark is bounded from below by TRISTAN, UA and CDF. If the top mass were below 30 GeV, the TRISTAN experiments should observe at their highest energies a predictable increase in the total cross section and similarly in differential distributions. This is not the case, hence 30 GeV is a safe lower limit. The

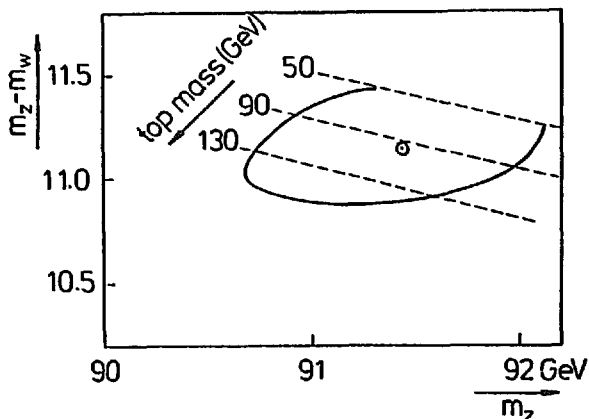


Figure 15: Constraints from  $p\bar{p}, e^+e^-$  and all fixed target experiments

searches at the  $p\bar{p}$  colliders for top sensitive final states yielded so far null results indicating that  $m_t$  is larger than about 60 GeV. On the other hand an upper limit on the top mass can only be obtained within the assumed theoretical framework. The radiative electroweak effects involve an  $m_t$  dependence, which is small, but measurable when all sectors are combined. The result can be summarized as follows :

$$m_t = 95 \begin{cases} +70 \\ -35 \end{cases} \text{ GeV}$$

•  $\sin^2 \Theta_W$

The value for the weak angle is dominated by the  $\nu$  quark sector. Integrating over all  $m_t$  one obtains :

$$\sin^2 \Theta_W = 0.229 \pm 0.004$$

There is no need to speculate right now about further consolidation of the electroweak theory or breakthroughs to new physics, since in the next few months several new results are expected : from CHARM II which has now a sample of 2000  $\nu e$  and  $\bar{\nu} e$  events, from UA and CDF on the weak boson masses and the top quark and in particular, from SLC and LEP. The applauded announcement of the observation of the first  $Z^0$  in the MARK II detector at SLC during this Workshop (there are already more than 30 events at the time

of finishing this write up) gives realistic hope that by summer the Z-mass will be known to about 300 MeV or better. Then, as obvious from Figure 15, the mass range of the top quark will be considerably narrowed down.

The new measurements will be precise enough to subject the electroweak theory to a strong test indeed.

## Acknowledgement

It is a pleasure to thank Paul Singer for the invitation to this Workshop and for the creative atmosphere. In preparing the talk I profitted from discussions with G.L. Fogli, K. Hagiwara, W. Hollik, H. Joos, H. Pietschmann and P. Zerwas. I like to thank my colleagues at KEK, F. Takasaki, K. Amako and T. Kamae for providing me their latest data.

## References

- [1] F. Abe et al.: Phys.Rev.Lett. **62** (1989) 1005
- [2] D. Haidt : Workshop on SPS Fixed Target physics 1982, CERN 83-02, p.63
- [3] M.C. Noecker et al.: Phys.Rev.Lett. **61** (1988) 310
- [4] W. Hollik : DESY 88-188 (Dec. 1988)
- [5] A. Sirlin : Phys.Rev. **D22** (1980) 971
- [6] J. Fujimoto, K. Kato and Y. Shimizu : Prog.Theor.Phys. **79** (1988) 701
- [7] T. Nozaki : Contribution to the Moriond Meeting, March 1989.  
L. Piilonen : Contribution to this Workshop, April 1989.  
G. Kim (AMY), S. Suzuki (TOPAZ), K. Ogawa (VENUS) : Contributions to the Topical Conference at KEK (Japan), May 1989.